3. K. Tanaka, A. Mikami, T. Ogura, K. Taniguchi, M. Yoshida, and S. Nakajima, *Appl. Phys. Lett.*, **48,** 1730 (1986).
4. S. Tanaka, H. Deguchi, Y. Mikami, M. Shiiki, and H. Kobayashi, *Proc. SID*, **28,** 21 (1987).
5. S. Tanaka, *J. Lumin.*, **40 & 41,** 20 (1988).
6. H. Ohnishi, R. Iwase, and Y. Yamasaki, in Digest of 1988 SID (Society for Information Display), 289, Los Angeles (1988).
7. H. Kobayashi, S. Tanaka, V. Shanker, M. Shiiki, and H. Deguchi, *J. Cryst. Growth*, **72,** 559 (1985).
8. B. D. Cullity, "Elements of X-Ray Diffraction," Addison-Wesley Pub. Co. Inc. (1956).
9. H. Yoshiyama, S. Tanaka, Y. Mikami, S. Ohshio, J. Nishiura, H. Kawakami, and H. Kobayashi, *J. Cryst. Growth*, **86,** 56 (1988).
10. H. Kasano, K. Megumi, and H. Yamamoto, *This Journal*, **131,** 1953 (1984).

Catalytic and Gas Sensing Characteristics in Pd-Doped SnO_2

J. G. Duh and J. W. Jou

Department of Materials Science and Engineering, National Tsing Hua University, Hsinchu, Taiwan, China

B. S. Chiou

Institute of Electronics, National Chiao Tung University, Hsinchu, Taiwan, China

ABSTRACT

A tin oxide based ceramic doped with ThO_2, MgO, and $PdCl_2$ is developed to detect the CO gas. The sensitivity of gas sensing is measured with respect to the relative resistance change in the ceramic matrix upon the introduction of the CO gas. Intermediate operating temperature is required for the gas sensing and high sensitivity is observed at 300°C. Metallic Pd is present in the sensing matrix after mixing in ethyl, while PdO shows up after sintering at 800°C. The presence of PdO enhances the CO gas sensitivity and the response rate. However, PdO tends to be transformed to Pd in the sensing process, which leads to the deterioration in the sensitivity. A post-oxidation treatment at 600°C proves to be effective in retaining PdO and high sensitivity without degradation can be obtained. In addition, a model in the gas sensing process is proposed.

SnO_2 is an n-type semiconductor. The chemisorption of a gaseous species on the SnO_2 surface can be treated as an electronic process in which charge transfer occurs between the adsorbed species and the semiconductor. For example, CO is oxidized on the SnO_2 surface, releases electrons to conduction band, and thus increases the conductivity. The employment of the change in the electrical conductivity of the semiconductor is widely used in gas sensing devices (1-8). In order to improve the sensing capabilities, several dopant materials have been added to the gas sensor. The effect from these materials has been evaluated (1, 9, 10). However, some detailed characteristics are still not clear, such as the state of the doped materials existing in the sensor, and the exact interaction between them and the matrix.

The influence of CO gas on the resistance change of SnO_2 sensor prepared with various amounts of $PdCl_2$ was investigated (11). An optimum $PdCl_2$ content around 2 weight percent (w/o) yielded the best response to CO gas. The purpose of this research is to study the sensing characteristic of SnO_2-based sensor in response to CO gas with the optimum contents of the catalyst. The sensor matrix is investigated with emphasis on the contribution of palladium and palladium oxide to the sensitivity. In addition, a possible sensing mechanism is proposed and discussed.

Experimental Procedures

Powders including SnO_2 and doping materials such as MgO, $PdCl_2$, and ThO_2 were mixed in ethyl alcohol and ball milled for 6h. The composition employed was 0.95 w/o MgO-1.90 w/o $PdCl_2$-5 w/o ThO_2-SnO_2. The mixed powders were dried at 150°C and the agglomerates were then crushed by an agate mortar. The pellet sample was made in a die under the pressure of 110 MPa. Pellets were sintered at 800°C for 45 min which was followed by air cooling. Gold was employed for the electrode by dc sputtering (Polaron E5100, Cheshire, England) with the Au thickness controlled at 2500Å with a thickness monitor. The electrode was annealed at 500°C for 15 min to obtain good contact with pellet samples.

X-ray diffractometer (Rikagu, Japan) was applied to investigate the phase in the fabricated sensor. ESCA (Electron Spectroscopy for Chemical Analysis, Perkin-Elmer PHI 1905, Minnesota) was also employed to study the oxidation state of palladium catalyst. The sensor resistance change in response to the introduction of CO gas was determined from the voltage across a resistor in series with the sample. Details of the resistance measurement setup are described elsewhere (11, 12).

Results and Discussion

Relative resistance change in gas sensing.—The relative resistance is defined as R/R_O, where R is the resistance at the instance of observation and R_O the initial resistance prior to gas introduction. The relative resistance at 3 min is chosen as the final response value. The sensitivity is then defined as (100%—final relative resistance value). Figure 1 shows the dependence of the relative resistance upon the temperature. Specimens were employed for 100 ppm CO gas testing at temperatures ranging from 100° to 350°C. The resistance of the specimen decreases as the temperature increases up to 300°C. It appears that there exists a lowest relative resistance value at 300°C.

The sensing response at different temperature is shown in Fig. 2. At higher temperature, the response rate is much enhanced. It takes less than 10s to reach the final relative resistance value for temperature higher than 300°C. The responses to different CO concentrations have also been measured and the results are presented in Fig. 3. At 300°C, higher sensitivity is obtained. The higher the CO concentration, the larger the relative resistance change. Figure 4 shows the response rate to different CO concentrations for sintered pellets at 300°C, which clearly demonstrates the fast response rate at 300°C. A saturated value of relative resistance change could be obtained within 10s after the introduction of CO gas. Table I lists the corresponding initial resistance for each gas test for different CO concentrations. These values were adjusted to assure that the sample possessed similar initial condition in each run, as a preliminary study revealed that the gas sensitivity would decrease when the initial resistance decreased (13).

It should be pointed out that in this study the sample was kept at 600°C in air for about 15 min before the next run. A series of tests showed that the relative resistance

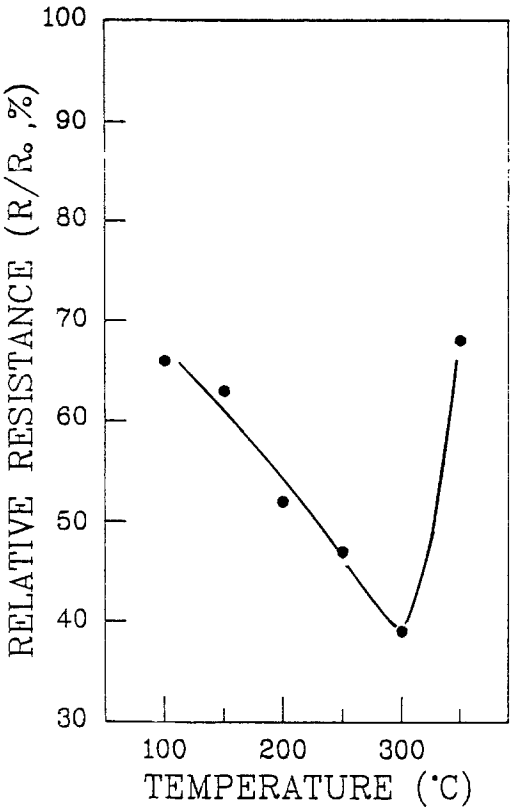

Fig. 1. The relative resistance of the sample 0.95 w/o MgO-1.90 w/o $PdCl_2$-5 w/o ThO_2-SnO_2 in response to 100 ppm CO gas as the function of temperature.

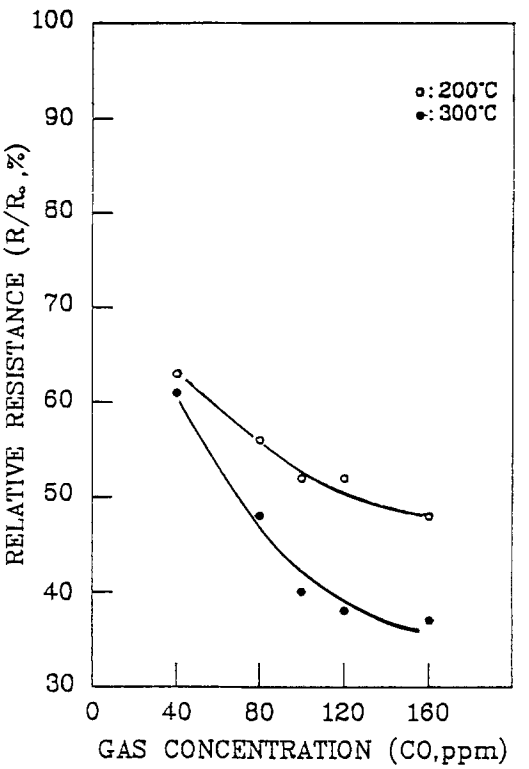

Fig. 3. The relative resistance of the sample 0.95 w/o MgO-1.90 w/o $PdCl_2$-5 w/o ThO_2-SnO_2 in response to different CO gas concentration.

maintained around 50% after the post-annealing treatment (13). However, for a sample without post-annealing a degradation in sensitivity was observed. The result of a repetitive test for the sample without 600°C oxidation treatment is shown in Fig. 5. Table II lists the corresponding initial resistance. The sensitivity decreases from 50 to 30% as the initial relative resistance decreases from 12.1 to 7.7 ± 0.2 MΩ. The degree of degradation in the sensitivity is, however, diminishing after several tests.

Pd-PdO transformation.—In discussing the role of the Pd catalyst in the sensing process, we note that $PdCl_2$ is soluble in ethyl alcohol and tends to be decomposed to Pd and Cl_2 around 500°C (14). An x-ray diffraction pattern revealed that metallic Pd existed in the dried precipitates of $PdCl_2$ in ethyl alcohol (13). To consider the possible phases for the constituents in the ceramic, we explore the free energies data listed below (15)

$$SnO_{2(s)} = SnO_{(s)} + 1/2\ O_{2(g)} \qquad [1]$$

$$\Delta G^\circ_1 = 73{,}240 + 10.43T \log T - 59.05T - 0.8 \times 10^{-3}T^2 - 2.48 \times 10^5/T$$

$$SnO_{2(s)} = Sn_{(s)} + O_2 \qquad [2]$$

$$\Delta G^\circ_2 = 140{,}180 - 51.52T$$

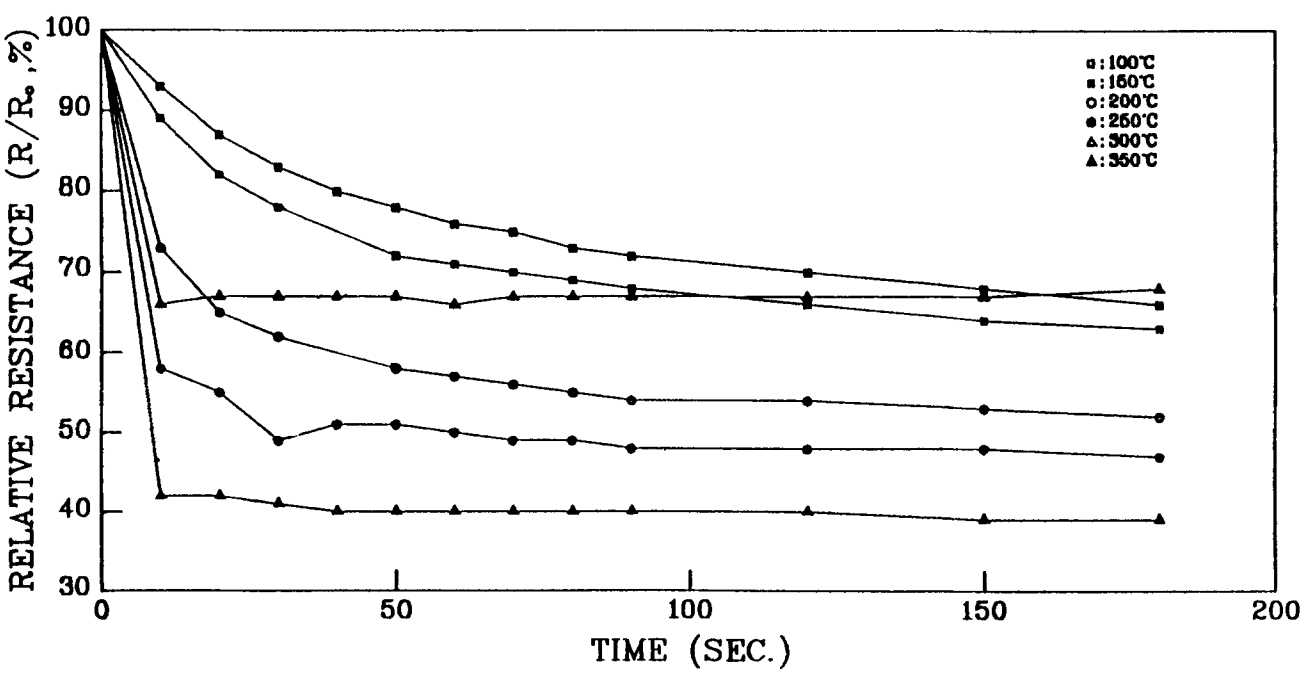

Fig. 2. The relative resistance of the sample 0.95 w/o MgO-1.90 w/o $PdCl_2$-5 w/o ThO_2-SnO_2 in response to 100 ppm CO gas

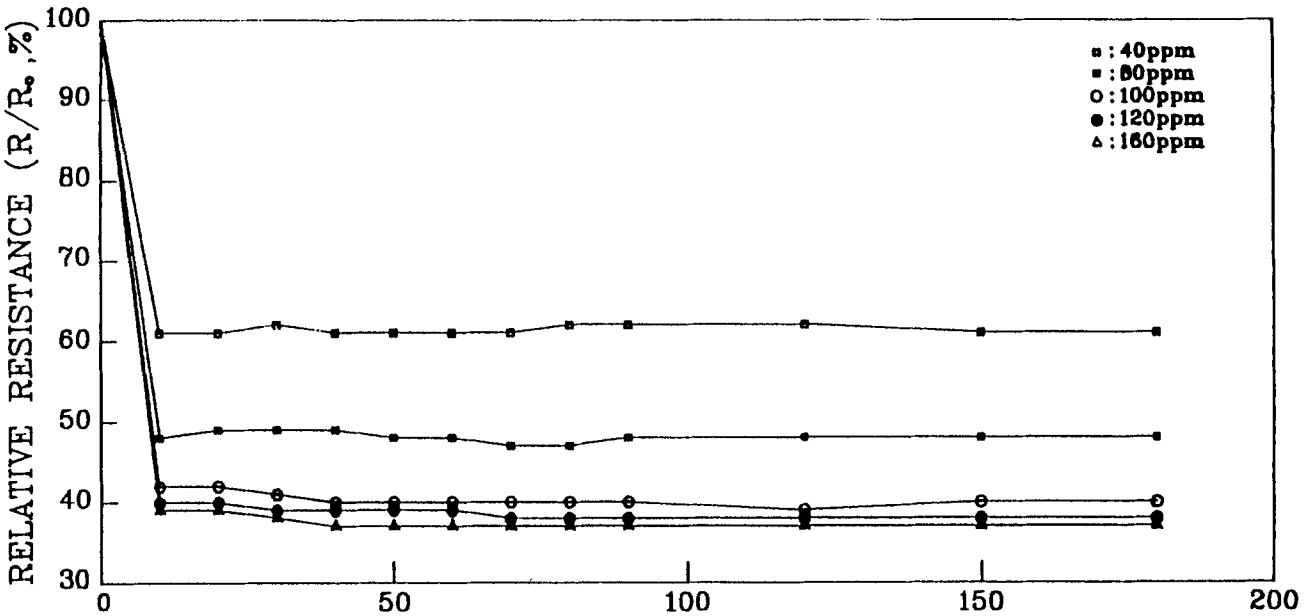

Fig. 4. The response of the sample 0.95 w/o MgO-1.90 w/o $PdCl_2$-5 w/o ThO_2-SnO_2 to different CO gas concentration at 300°C as the function of time.

$$ThO_2(s) = Th_{(s)} + O_{2(g)} \quad [3]$$
$$\Delta G^\circ_3 = 293{,}400 + 1.61T \log T - 47.7T$$

$$MgO_{(s)} = Mg_{(s)} + 1/2\ O_{2(g)} \quad [4]$$
$$\Delta G^\circ_4 = 144{,}350 + 2.95T \log T - 33.95T$$

$$Pd_{(s)} + 1/2\ O_{2(g)} = PdO_{(s)} \quad [5]$$
$$\Delta G^\circ_5 = -22{,}400 - 5.75T \log T + 36.9T$$

For a temperature lower than 1000°C, the values of ΔG°_1, ΔG°_2, ΔG°_3, ΔG°_4 given above are all greater than zero, which indicate that SnO_2, ThO_2, MgO are stable phases during the sintering process. However ΔG°_5 is greater than zero at temperatures higher than 890°C and less than zero at temperatures lower than 890°C. Hence, PdO is stable at temperatures lower than 890°C and Pd prevails at temperatures higher than 890°C. It is interesting to note that Pd could be oxidized at a lower temperature, while PdO reduced at a higher temperature. More thermodynamic data involving SnO_2, SnO, Pd, PdO, ThO_2, and MgO are presented as follows

$$SnO_{2(s)} + Pd_{(s)} = Sn_{(s)} + PdO_{(s)} + 1/2\ O_{2(g)} \quad [6]$$
$$\Delta G^\circ_6 = 117{,}780 - 5.75T \log T - 14.62T$$

$$SnO_{2(s)} + Pd_{(s)} = SnO_{(s)} + PdO_{(s)} \quad [7]$$
$$\Delta G^\circ_7 =$$
$$50{,}840 - 4.68T \log T - 22.15T - 0.8 \times 10^{-3}T^2 - 2.48 \times 10^5/T$$

$$ThO_{2(s)} + Pd_{(s)} = Th_{(s)} + PdO_{(s)} + 1/2\ O_{2(g)} \quad [8]$$
$$\Delta G^\circ_8 = 271{,}000 - 4.14T \log T - 10.8T$$

$$MgO_{(s)} + Pd_{(s)} = Mg_{(s)} + PdO_{(s)} \quad [9]$$
$$\Delta G^\circ_9 = 121{,}950 - 2.8T \log T + 2.95T$$

When the temperature is less than 890°C, ΔG°_6, ΔG°_7, ΔG°_8, ΔG°_9 are all greater than zero, thus it is impossible for the reactions in Eq. [6], [7], [8], and [9] to move toward the right-hand side.

To have the possibility of observing the existing phases in this material, two special specimens were prepared. One was SnO_2 + 20 w/o $PdCl_2$, another ThO_2 + 25 w/o $PdCl_2$ + 10 w/o MgO. Figures 6 and 7 present the x-ray diffraction pattern of specimens SnO_2 + $PdCl_2$ and ThO_2 + $PdCl_2$ + MgO, respectively, after mixing and calcination at 800° and 900°C. Pd showed up after drying, which was an indication

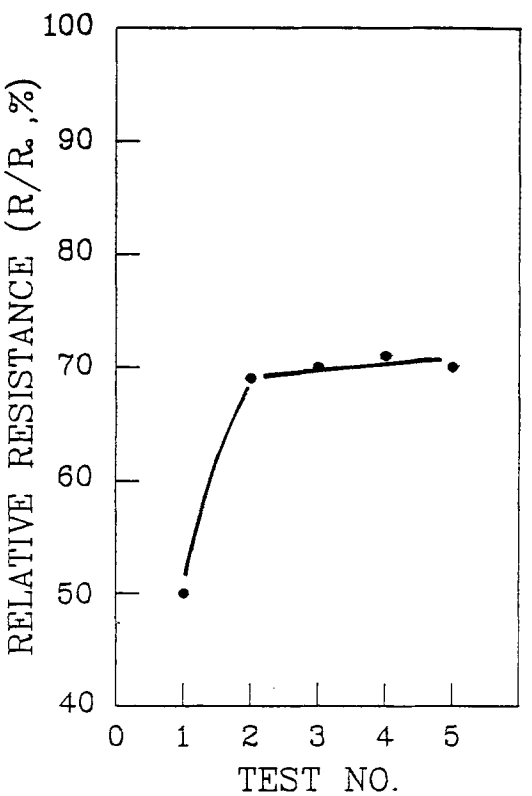

Fig. 5. The relative resistance of repetitive test to 100 ppm CO at 300°C for the sample 0.95 w/o MgO-1.90 w/o $PdCl_2$-5 w/o ThO_2-SnO_2 without post-oxidation treatment.

Table I. The initial resistance in the sensing ceramic corresponding to Fig. 4

CO concentration (ppm)	40	80	100	120	160
R_o (MΩ)	14.1	13.9	13.5	12.8	15.3

Table II. The initial resistance in the sensing ceramic corresponding to Fig. 5

Test no.	1	2	3	4	5
R_o (MΩ)	12.1	7.9	7.6	7.4	7.7

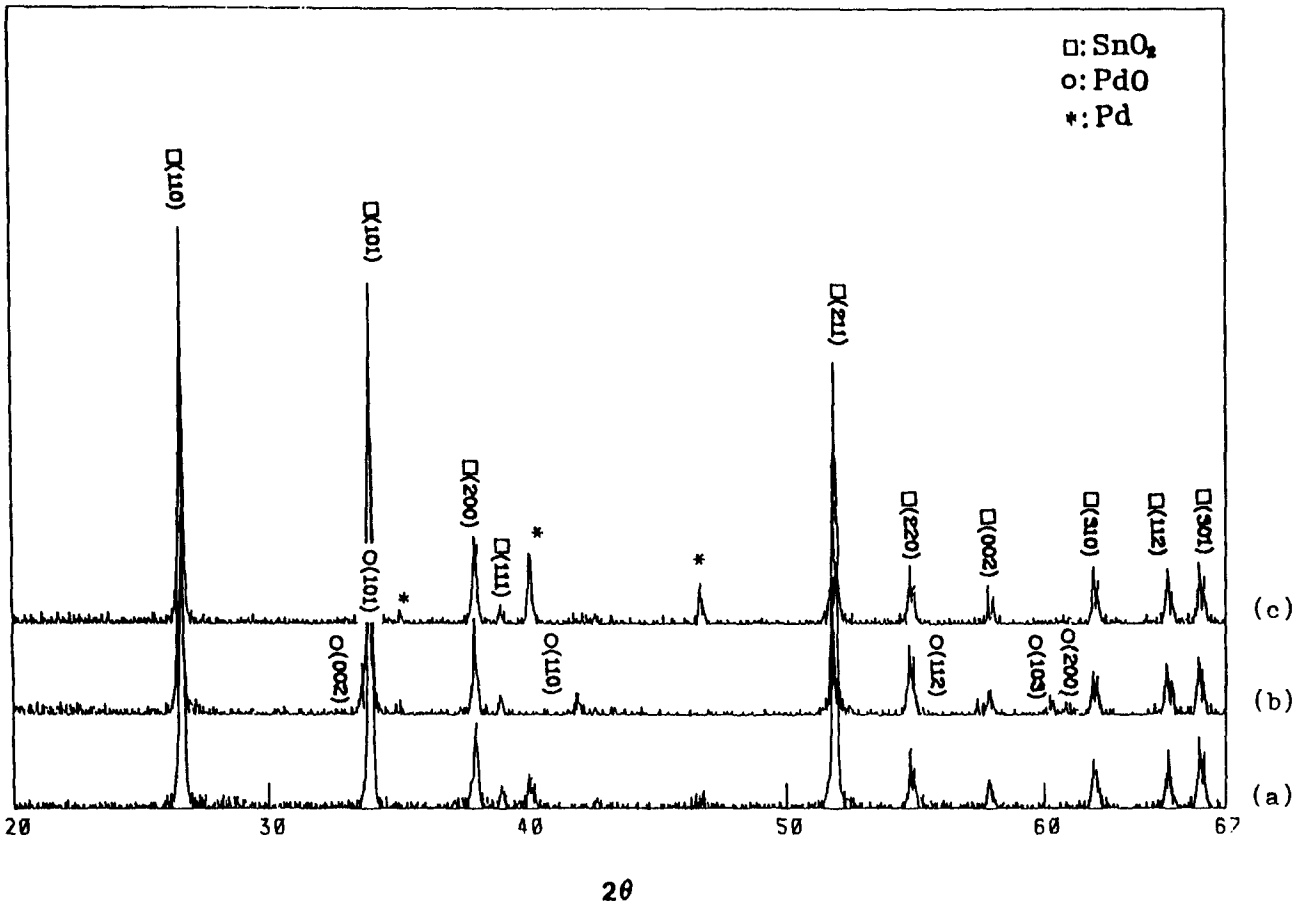

Fig. 6. X-ray diffraction pattern of the sample 20 w/o $PdCl_2$-SnO_2 (a) dried after mixing, (b) calcined at 800°C, (c) calcined at 900°C

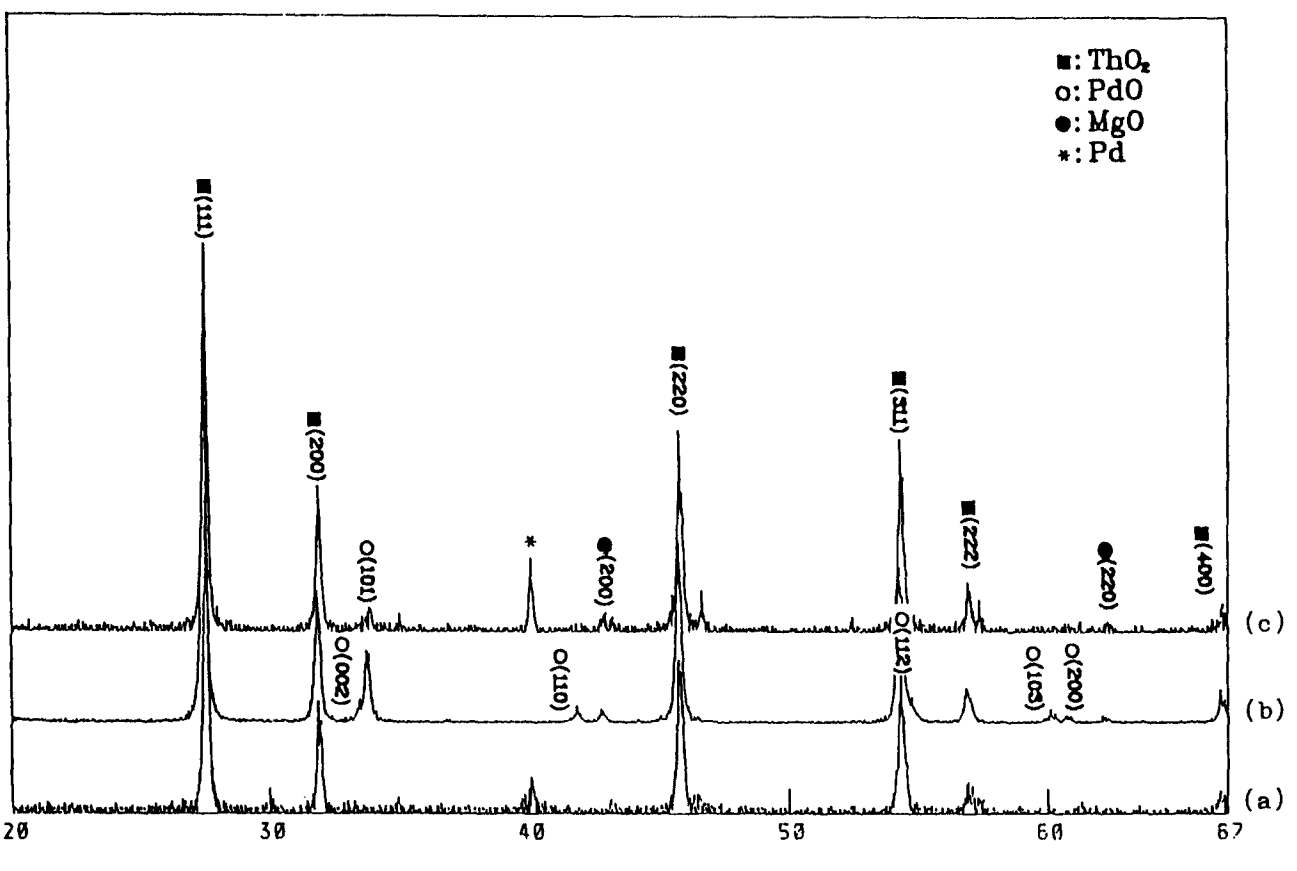

Fig. 7. X-ray diffraction pattern of the sample 25 w/o $PdCl_2$-10 w/o MgO-ThO_2 (a) dried after mixing, (b) calcined at 800°C, (c) calcined at 900°C

of Pd precipitation from the solution of $PdCl_2$ in ethyl alcohol. This is the advantage of using $PdCl_2$ instead of pure Pd as our approach offers the possibility of having Pd precipitate homogeneously dispersed around the stable oxide particles. From Fig. 6 and 7, PdO is observed at calcination temperature 800°C, while Pd is found in the dried powders after mixing and also at calcination temperature 900°C. There exist no extra peaks, which implies that no new compounds are formed due to interaction among the parent components. In fact, ESCA analysis as shown in Fig. 8, reveals that the sample surface is covered with PdO when sintered at 800°C, as the peaks in Fig. 8(c) are identified to be Pd^{+2}. A similar observation is obtained for the sample sintered at 900°C and followed by rapid cooling to room temperature in less than 20s, although the x-ray diffraction indicates that the bulk is still Pd on the basis of Fig. 7. It should be pointed out that relatively speaking x-ray diffraction is employed for bulk analysis, whereas ESCA is for surface characterization. According to the data in Fig. 8, it can be confirmed that the originally doped $PdCl_2$ is transformed to PdO on the surface of the sample after sintering. However, whether PdO will participate in the oxidation of CO or catalyze the sensing behavior of SnO_2 is another focal point to be probed.

A new sintering process was designed to investigate the interaction between PdO and SnO_2. Samples were first sintered at 900°C for 30 min in air and then annealed at 500°C for 1, 5, 10, and 15h, respectively. Such an annealing process was intended to oxidize Pd. The amount of PdO increases with the annealing time as shown in Fig. 9. Peaks of Pd become smaller after 15h annealing, while enhanced peaks of PdO show up. This indicates that more Pd is transformed to PdO as the annealing time increases. Samples of various annealing time were tested in response to 100 ppm CO at 300°C. Figure 10 shows that higher sensitivity is obtained for longer annealing time, in which more PdO is present.

Samples after oxidation for 15h and those without $PdCl_2$ (*i.e.*, no PdO) were then employed in a series of tests in response to 100 ppm CO at 200° and 300°C, as shown in Fig. 11. No data are available for the sample without $PdCl_2$ at 200°C, since such sample exhibits no response to CO gas at 200°C based on thermodynamical considerations. The influence of PdO on the CO sensitivity can be further appreciated with the aid of Fig. 11. It is apparent that for sample doped with $PdCl_2$ and oxidized for 15h, the response rate to 100 ppm CO at 300°C is much faster than the one without $PdCl_2$ dopant.

Basically, the process in gas sensing is an oxidation-reduction process. CO is converted to CO_2 in the presence of SnO_2. The resistance change before and after CO inlet is employed for the CO gas detection. After sintering, doped $PdCl_2$ is transformed to PdO, which, in turn, enhances the reaction for CO to CO_2. The resistance change is detected only when oxidation-reduction occurs on the sample surface. It is beneficial to know which components existing in the sensor participate in the conversion of CO to CO_2. More useful information could be derived from thermodynamics. The free energy equations associated with CO, ThO_2, MgO, SnO_2, PdO are listed below (15)

$$CO_{(g)} + ThO_{2(s)} = CO_{2(g)} + Th_{(s)} + 1/2\ O_{2(g)} \qquad [10]$$
$$\Delta G^\circ_{10} = 225{,}900 + 1.61T \log T - 26.95T$$

$$CO_{(g)} + MgO_{(s)} = CO_{2(g)} + Mg_{(s)} \qquad [11]$$
$$\Delta G^\circ_{11} = 76{,}850 + 2.95T \log T - 13.2T$$

$$CO_{(g)} + SnO_{2(s)} = CO_{2(g)} + Sn_{(s)} + 1/2\ O_{2(g)} \qquad [12]$$
$$\Delta G^\circ_{12} = 72{,}680 - 30.77T$$

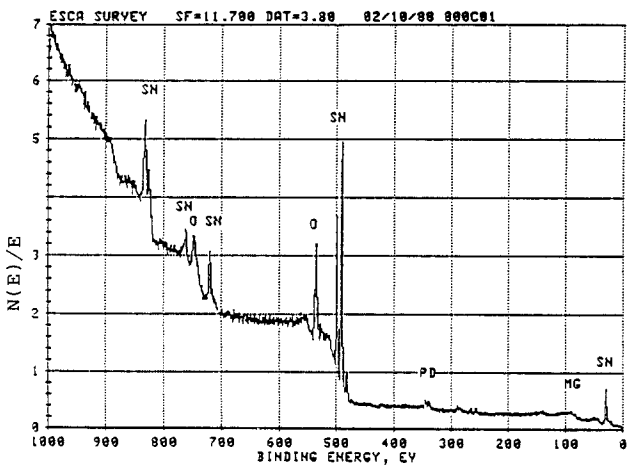

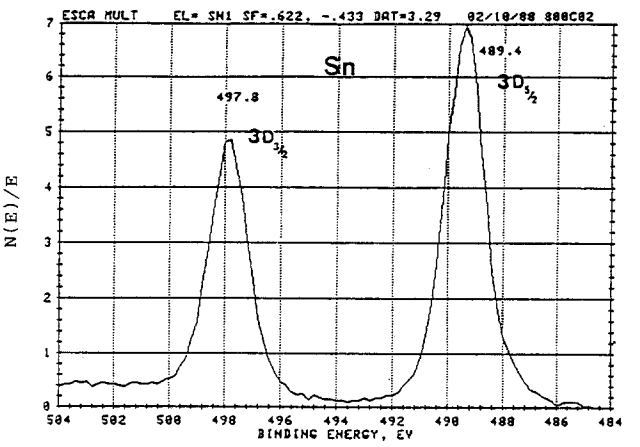

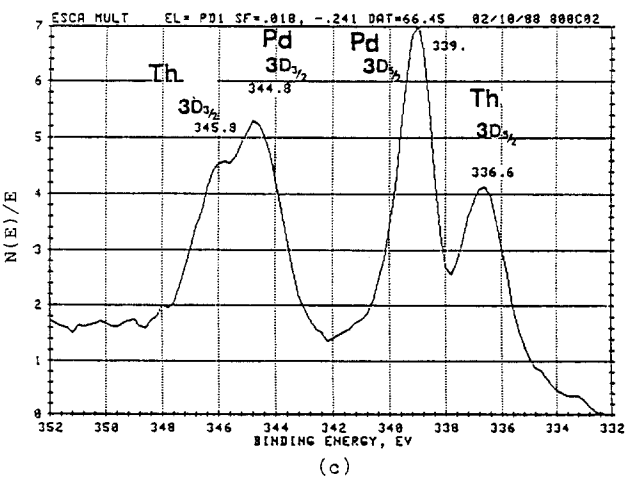

Fig. 8. ESCA spectrum for the sample 0.95 w/o MgO-1.90 w/o $PdCl_2$-5 w/o ThO_2-SnO_2 sintered at 800°C (a) single scan, (b) multiple scan for Sn, (c) multiple scan for Pd and Th.

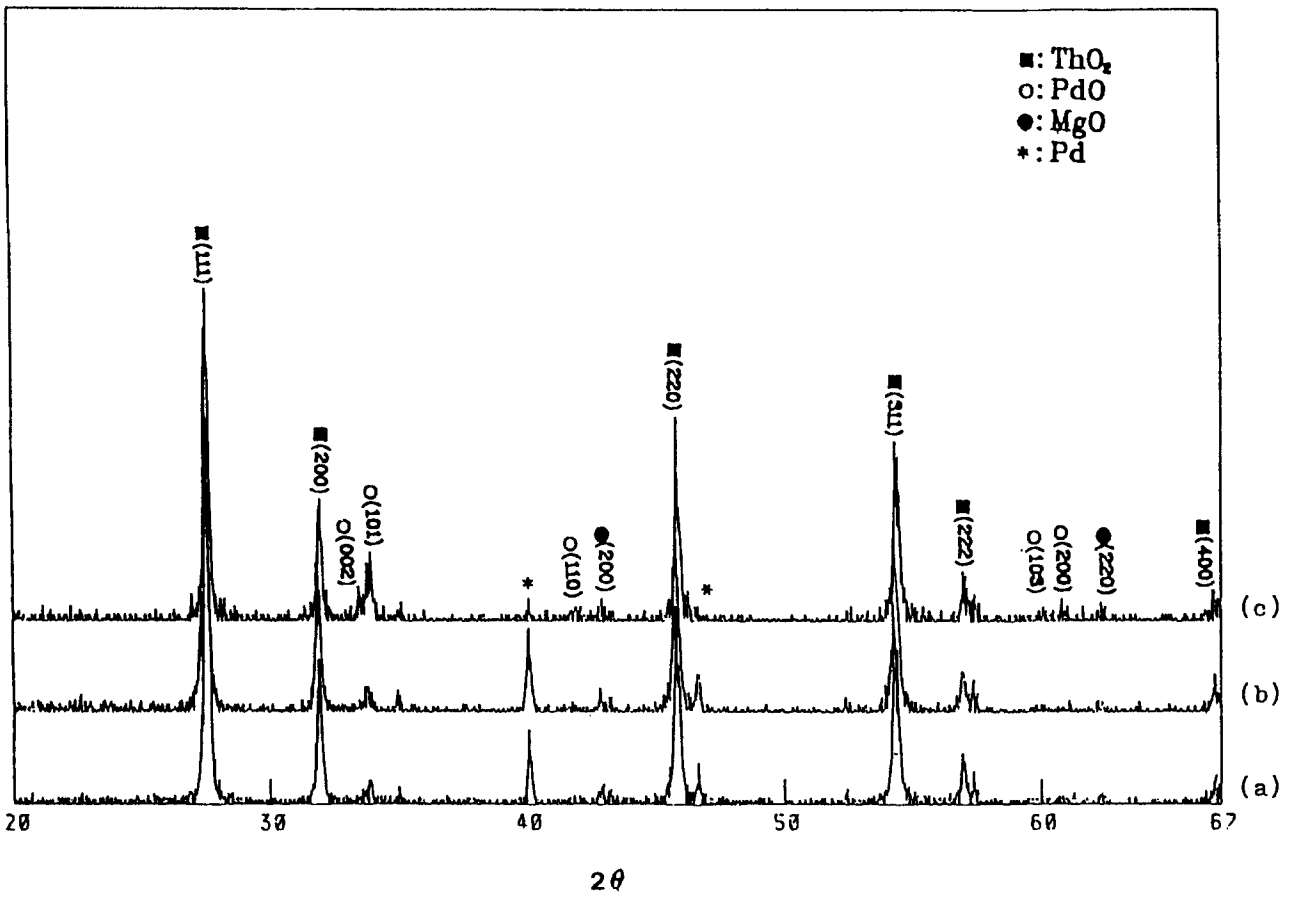

Fig. 9. X-ray diffraction pattern of the sample 10 w/o MgO − 25 w/o $PdCl_2$-ThO_2 calcined at 900°C and then oxidized at 500°C for various time (a) 0h, (b) 1h, (c) 15h.

$$CO_{(g)} + SnO_{2(s)} = CO_{2(g)} + SnO_{(s)} \quad [13]$$
$$\Delta G^\circ_{13} = 5{,}740 + 10.43T \log T - 38.3T - 0.8 \times 10^{-3}T^2 - 2.48 \times 10^5/T$$

$$CO_{(g)} + PdO_{(s)} = CO_{2(g)} + Pd_{(s)} \quad [14]$$
$$\Delta G^\circ_{14} = -45{,}100 + 5.75T \log T - 16.15T$$

For the operating temperature below 500°C, ΔG°_{10}, ΔG°_{11}, and ΔG°_{12} are all greater than zero, and the corresponding reactions are not feasible. However, ΔG°_{13} is less than zero at temperature above 230°C, and it is possible that SnO_2 is reduced to SnO by CO gas. At the operating temperature below 500°C, it is possible for PdO to oxidize CO, since ΔG°_{14} is less than zero. Once PdO is reduced at 200° or 300°C, the reoxidation for Pd to PdO is decelerated. As shown in Fig. 9 for specimen oxidized at 500°C for 15h, there still exists peaks for Pd, even though these powdered samples have larger surface energy than sintered pellets. For SnO, it is thermodynamically possible to be oxidized to SnO_2. It is reported that the reoxidation for SnO to SnO_2 is fairly fast (1).

More information from thermodynamics about SnO_2, PdO, and H_2 is listed below (15) to explain the interaction among various species

$$SnO_{2(s)} + H_{2(g)} = SnO_{(s)} + H_2O_{(g)} \quad [15]$$
$$\Delta G^\circ_{15} = 15{,}990 + 14.91T \log T - 61.26T$$

$$PdO_{(s)} + H_{2(g)} = Pd_{(s)} + H_2O_{(g)} \quad [16]$$
$$\Delta G^\circ_{16} = -34{,}850 + 10.23T \log T - 39.11T$$

At 320°C, thermodynamics predict that SnO_2 cannot be reduced to SnO, but PdO can. A spill-over effect is thus proposed

$$PdO(\ \ ) + H_2 = PdO(H_2) \quad [17]$$

$$PdO(H_2) + SnO_2 = PdO(\ \ ) + SnO + H_2O \quad [18]$$

where PdO( ) is a vacant site for adsorption on PdO and $PdO(H_2)$ presents physisorbed H_2 on PdO.

PdO itself could also be reduced to Pd, *i.e.*

$$PdO + H_2 = Pd + H_2O \quad [19]$$

After annealing in H_2, phases existing in this sample are MgO, ThO_2, SnO, and Pd. At the beginning, the increase of the resistance of the sample is due to the reoxidation of

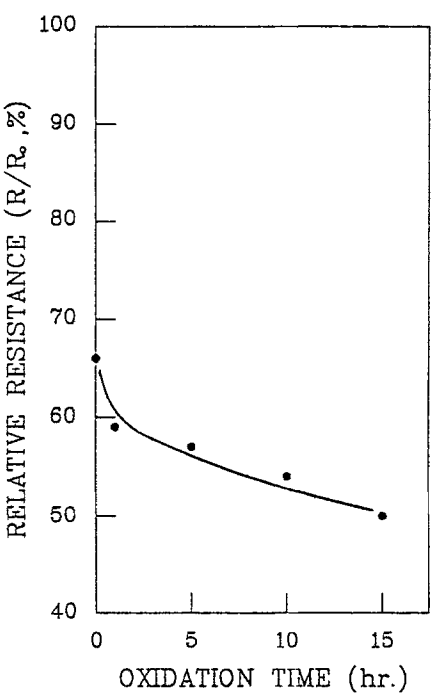

Fig. 10. The relative resistance of the sample 0.95 w/o MgO-1.90 w/o $PdCl_2$-5 w/o ThO_2-SnO_2 sintered at 900°C and then oxidized at 500°C for various times.

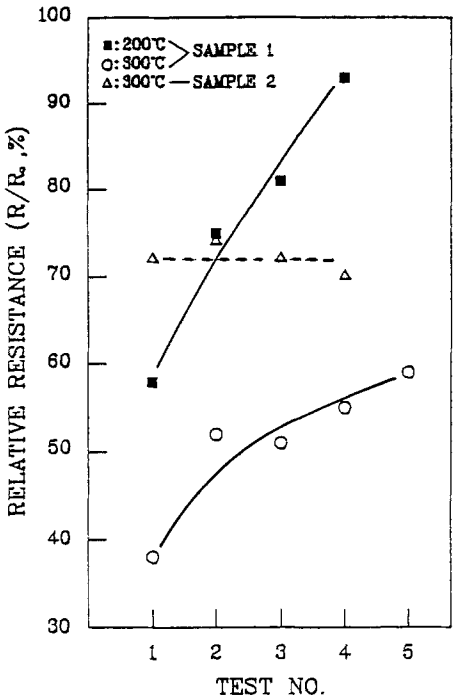

Fig. 11. The relative resistance of repetitive gas test to 100 ppm CO. Sample 1: $PdCl_2$-doped SnO_2 sample oxidized for 15h. Sample 2: $PdCl_2$-free SnO_2.

SnO. Both hydrogen and carbon monoxide are reducing gases, and possess similar properties. Samples without PdO exhibit no response to CO gas at 200°C, as indicated in Fig. 11.

On the basis of the above data a model for sensing process in this study is proposed as follows

$$PdO(\ ) + CO = PdO(CO) \quad [20]$$

$$PdO(CO) + SnO_2 = PdO(\ ) + SnO + CO_2 \quad [21]$$

$$SnO + 1/2\ O_2 = SnO_2\text{: fast} \quad [22]$$

$$PdO(CO) + PdO = PdO(\ ) + Pd + CO_2 \quad [23]$$

$$Pd + 1/2\ O_2 = PdO\text{: slow} \quad [24]$$

Gas detection is through resistance change, and the phenomenon occurs when chemisorption takes place. PdO tends to trap CO and such trapped CO diffuses inward and reacts with SnO_2. It may also diffuse to other PdO and react with each other. However, the reoxidation rates at 200° or 300°C are much different since reaction in Eq. [22] is fast, whereas that in Eq. [24] is slow. This explains the unrecoverable and recoverable regions in the resistance change as shown in Fig. 5 and Table II. At low temperature 200°C, the dominating reaction is Eq. [23], while Eq. [21] predominates at higher temperature above 300°C. That is the reason why there is no equilibrium relative resistance values to 100 ppm CO in the repetitive gas test at 200°C. However, at 300°C, a nearly equilibrium is reached, as indicated in Fig. 11. More evidence for the existance of Pd and SnO could be obtained from x-ray diffraction result. Figure 12 shows the x-ray diffraction pattern for samples sintered at 800°C and followed by annealing in CO at 200° and 300°C. As compared to that for samples only after sintering at 800°C (13), a small extra peak appears near $2\theta = 40$°C at both 200° and 300°C, as shown in Fig. 13 on the basis of the step scan in x-ray diffraction. The peak near 40° was identified as Pd. Another peak around $2\theta = 29.3$°, as seen in Fig. 14, was identified to be SnO, which showed up for sintered sample annealed at 300°C, but not at 200°C.

It is argued that the deterioration in the sensor system consisting of $SnO_2 + PdCl_2 + MgO + ThO_2$ is attributed to the reduction of PdO to Pd by the reducing gas CO. The presence of PdO enhances the sensitivity of CO detection as shown in Fig. 10 and 11. However, the reduction of PdO

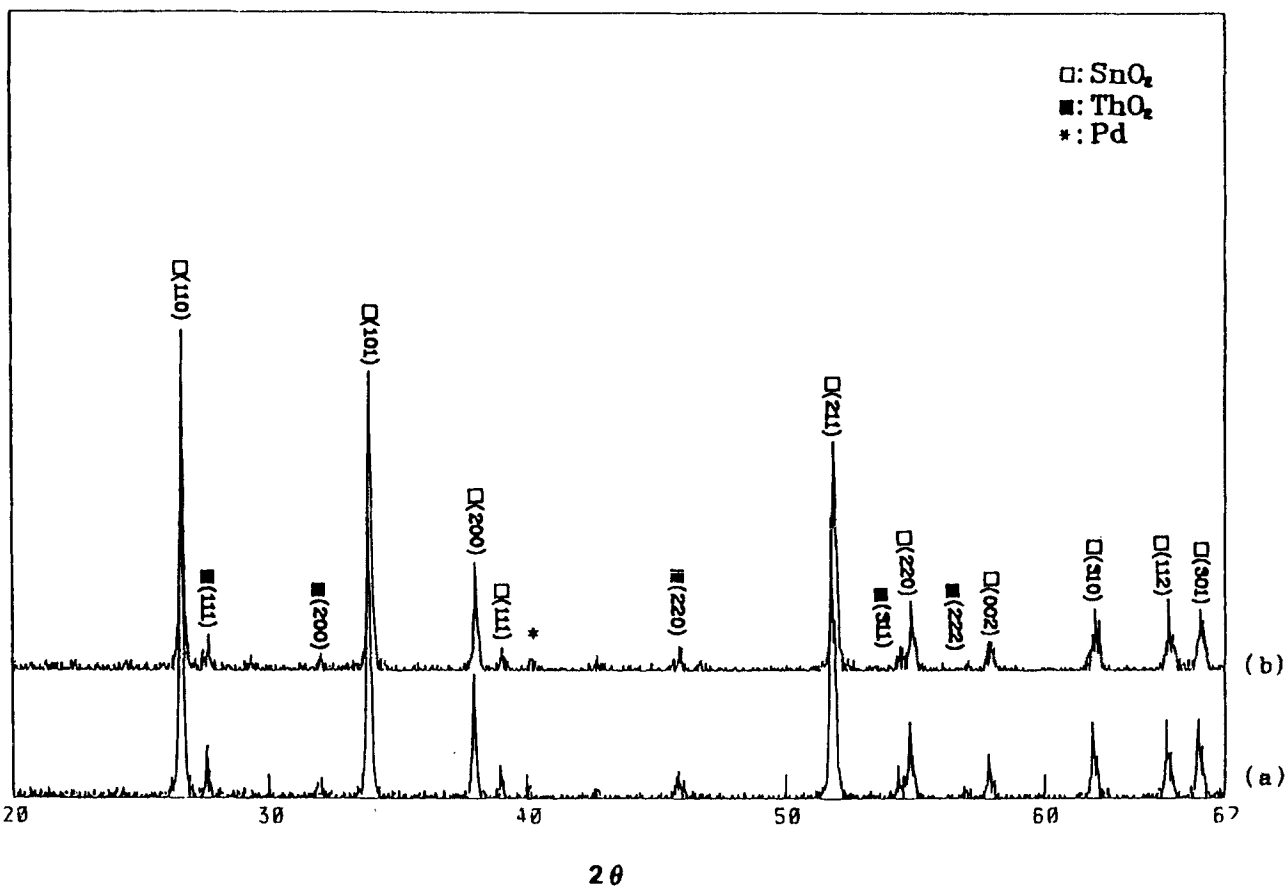

Fig. 12. X-ray diffraction pattern of the sample 0.95 w/o MgO-1.90 w/o $PdCl_2$-5 w/o ThO_2-SnO_2 sintered at 800°C and annealed in CO atmosphere at (a) 200°C, (b) 300°C.

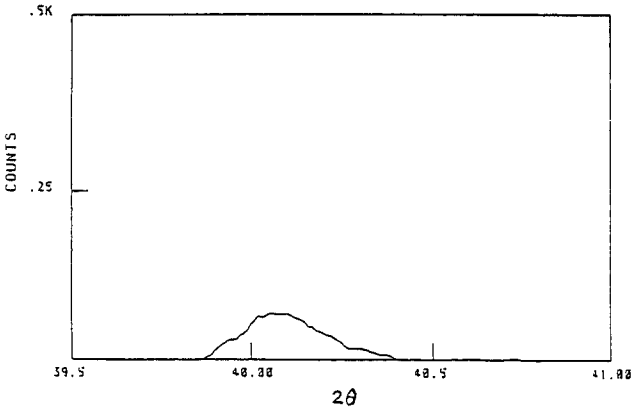

Fig. 13. Step scan by x-ray for the sample 0.95 w/o MgO-1.90 w/o $PdCl_2$-5 w/o ThO_2-SnO_2 annealed at 200°C in CO atmosphere, the condition for step scan: sampling, 0.008°; fixed time, 4s, the peak is identified as Pd.

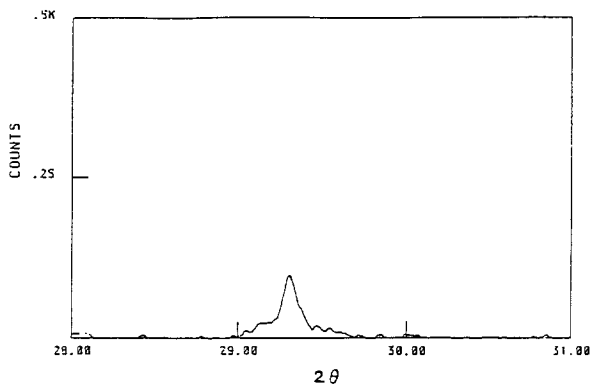

Fig. 14. Step scan by x-ray for the sample 0.95 w/o MgO-1.90 w/o $PdCl_2$-5 w/o ThO_2-SnO_2 annealed at 300°C in CO atmosphere, the peak is identified as SnO.

to Pd retards the sensitivity as indicated in Fig. 5 and 11. With post-oxidation treatment at 600°C no change of sensitivity is observed as stated before, while the sensitivity decreases from 50 to 30% as shown in Fig. 5 for sample without post-oxidation, in which Pd retains the metallic state. A further examination in Fig. 11 reveals that the sample without $PdCl_2$ dopant exhibits 30% sensitivity, which is comparable to the result in Fig. 5. The decrease of sensitivity in $PdCl_2$ doped sample, as indicated in Fig. 11, is due to the transformation of PdO to Pd. It is not thermodynamically feasible for Pd to be reoxidized to PdO at low temperature around 200° or 300°C and the sensitivity is thus decreased. However, the employment of post-oxidation at 600°C promotes the transformation of Pd back to PdO and higher sensitivity without decay is obtained.

Summary

1. Intermediate operating temperature is required for the CO gas sensing in 0.95 w/o MgO-1.90 w/o $PdCl_2$-5 w/o ThO_2-SnO_2 ceramic. Higher sensitivity and fast response rate is observed at 300°C.

2. Metallic Pd is observed in the sensing matrix after mixing in ethyl alcohol, while PdO shows up after sintering at 800°C.

3. The presence of PdO enhances the CO gas sensitivity and the response rate.

4. PdO tends to be reduced to Pd in the sensing process, which leads to the deterioration in the sensitivity. A post-oxidation treatment at 600°C proves to be effective in retaining PdO and higher sensitivity without degradation is thus obtained.

5. A model for the reactions in the gas sensing process is proposed as follows

$$PdO(\ \ ) + CO = PdO(CO)$$

$$PdO(CO) + SnO_2 = PdO(\ \ ) + SnO + CO$$

$$SnO + 1/2\ O_2 = SnO_2\text{: fast}$$

$$PdO(CO) + PdO = PdO(\ \ ) + Pd + CO$$

$$Pd + 1/2\ O_2 = PdO\text{: slow}$$

At low temperature, the controlling reaction lies in the fourth equation, while the second equation predominates at higher temperatures above 300°C.

Manuscript submitted Oct. 24, 1988; revised manuscript received March 27, 1989.

National Tsing Hua University assisted in meeting the publication costs of this article.

REFERENCES

1. M. Nitta and M. Haradome, *IEEE Trans. Electron Devices*, **ED-26,** 219 (1979).
2. H. Windischmann and P. Mark, *This Journal*, **126,** 627 (1979).
3. P. Tischez, H. Pink, and L. Treitinger, *Jpn. J. Appl. Phys.*, **19,** 513 (1980).
4. P. K. Clifford and D. T. Tuma, *Sensors and Actuators*, **3,** 233 (1982/1983).
5. T. Oyabu, *J. Appl. Phys.*, **53,** 2785 (1982).
6. T. Oyabu, T. Osawa, and T. Kurobe, *ibid.*, **53,** 7125 (1983).
7. S. Kanefusa, M. Nitta, and M. Haradome, *ibid.*, **52,** 498 (1981).
8. M. Nitta, S. Kanefusa, S. Ohtani, and M. Haradome, *J. Electron. Mater.*, **13,** 15 (1984).
9. M. Nitta and M. Haradome, *ibid.*, **8,** 571 (1979).
10. M. Nitta and M. Haradome, *ibid.*, **9,** 727 (1980).
11. B. S. Chiou, J. J. Lee, and J. G. Duh, *ibid.*, **17,** 485 (1988).
12. J. J. Lee, M. S. Dissertation, National Tsing Hua University, Hsinchu, Taiwan (1986).
13. J. W. Jou, M. S. Dissertation, National Tsing Hua University, Hsinchu, Taiwan (1988).
14. A. Rose and E. Rose, "The Condensed Dictionary," 7th ed., p. 703, Van Nostrand Reinhold Co. (1966).
15. O. Kubaschewski, E. L. Evans, and C. B. Alcock, in "Metallurgical Thermochemistry," 4th ed., Pergamon Press, Edinburg (1967).